

Dependence of Low Frequency Waves on Magnetic Field Strength in Hollow Cathode Plume

IEPC-2019-249

*Presented at the 36th International Electric Propulsion Conference
University of Vienna, Austria
September 15–20, 2019*

Marcel P. Georjin*, Benjamin A. Jorns[†] and Alec D. Gallimore[‡]
University of Michigan, Ann Arbor, MI 48109

The formation of quasi-coherent plasma structures in the plume of a hollow cathode is investigated with varying magnetic field strength. In particular, the claim that rotating modes that grow in the presence of a magnetic field are the same as the ionization instability associated with the plume mode is assessed experimentally. An experiment is conducted at high propellant flow rate (spot mode), where increasing the magnetic field causes both an azimuthal ($m = 1$) mode and a longitudinal ($m = 0$) mode to form. The rotating instability is consistent with an anti-drift wave description in the limit of low-magnetic field strength. The origin of the $m = 0$ remains unclear, however by evaluating a proposed onset criterion for the ionization instability finds that under these conditions, it should be damped out. At a second condition with a low propellant flow rate (plume mode), a quasi-coherent instability forms and propagates longitudinally. This wave is shown to be consistent with the ionization instability commonly observed in plume mode by evaluating the same onset criterion. As the magnetic field is increased, the amplitude of the instability is reduced. The coherent structures in spot mode are shown to have opposing trends with magnetic field and have different propagation velocities than that of the ionization wave. These differences are used to argue that these waves are likely different instabilities with separate growth and onset criteria.

*Ph.D Candidate, Applied Physics Program, georjinm@umich.edu

[†]Assistant Professor, Department of Aerospace Engineering

[‡]Robert J. Vlasic Dean of Engineering, the Richard F. and Eleanor A. Towner Professor of Engineering, and Arthur F. Thurnau Professor of Aerospace Engineering

Nomenclature

A_o	= Cathode orifice area
c_s	= Ion sound speed
E	= Electric field
I_{sat}	= Ion saturation current
I_{dc}	= Discharge current
k	= Wave vector
m_e	= Electron mass
m_i	= Ion mass
\dot{m}	= Mass flow rate
n	= Plasma density
p_k	= Wave momentum
q	= Unit charge
T_e	= Electron temperature
T_i	= Ion temperature
u_e	= Electron drift velocity
u_i	= Ion drift velocity
v_e	= Electron thermal velocity
V_f	= Floating potential
Φ	= Plasma potential
ν	= Total collision frequency
ν_{an}	= Anomalous collision frequency
ν_{ion}	= Ionization frequency
γ_{IAT}	= Turbulence growth rate
γ_{ion}	= Response rate of ionization to temperature
ω_r	= Real frequency of oscillation
ω_i	= Imaginary frequency of oscillation

I. Introduction

The hollow cathode plume is known to be subject to plasma instabilities that can drive steady and large-scale transient behavior in their discharges. Ion acoustic turbulence (IAT) is known to play a prominent role in establishing the steady-state electron resistivity.¹⁻⁷ As indicated by recent experimental measurements and simulations, it is thought to be the dominant contributor to the onset of the ionization instability observed in plume mode cathode operation.⁸⁻¹¹ The onset of plume mode is often identified with global parameters, such as keeper voltage oscillations and increased erosion but is also well known to be characterized by large plasma potential, density and light fluctuation that are quasi-coherent.¹²⁻¹⁶ While these waves can be readily measured in unmagnetized plumes of hollow cathodes, the introduction of an axial magnetic field, like those found in Hall thrusters where the cathode is centrally mounted, can complicate the presentation of these instabilities. Although ion acoustic waves have been measured in the cathode plume of a Hall thruster,^{17,18} the ionization instability has never been identified; however this may be because the plume mode is typically avoided when operating a Hall thruster for performance and system life-time considerations.¹⁹ In fact, it is unclear whether the presence of a magnetic field in the cathode plume could allow for the conditions necessary for the plume mode to onset.

For more detailed research on hollow cathode physics, these devices are often tested in standalone configurations.^{20,21} These experiments will commonly employ an applied axial magnetic field to better simulate the conditions found in Hall thrusters. Visually, with increasing magnetic field strength the shape of the cathode plume can change drastically, from a small spot at the keeper exit, to an extended plasma column. Along with the magnetic field comes rotating modes, that have also been observed in Hall thrusters with high-speed camera measurements.²² These so-called cathode spokes are thought to be the result of an anti-drift wave that could lead to the erosion of Hall thruster pole cover surfaces and may be involved in electron transport across magnetic field lines in this region of the thruster.

The presence of these rotating modes, and the possibility that they may influence transport in the cathode region of Hall thrusters, presents a challenge for simulating these cathodes computationally. Typically, these numerical models will use a r-z domain and include quasi-3D effects, however they cannot resolve azimuthal inhomogeneities.^{6,8,9} Recent numerical simulations that include the effects of the non-classical resistivity from turbulence show that, in the presence of a magnetic field, the large-plasma potential oscillations commonly associated with the plume mode are able to propagate and exist in the plume of the cathode. Although qualitative and quantitative agreement has been found between this model and experimental measurements, they do not capture these rotating instabilities which are known to dominate the cathode plume in the presence of an axial magnetic field. Qualitative indications from experiments seem to suggest that the magnetic field might suppress the onset of the axial plume mode instability in favor of the azimuthal instability;²² however, there are no detailed experimental measurements that show they do not coexist.

Given the deleterious effects of these instabilities to performance and the inconclusive nature of recent numerical simulations on the matter, there is an apparent need for precise experimental measurements of cathode instabilities under the influence of a magnetic field examining the presence of axial and azimuthal modes. To this end, we have organized this article in the following manner. First, we present an overview of the various instabilities that are known to exist in hollow cathode plumes. Next we describe our experimental configuration, along with diagnostics we have employed to measure plasma waves. To follow, is a presentation of the experimental results from two conditions, one in spot mode and another plume mode with varying magnetic field strength. We then discuss these results by comparing and contrasting the structures formed in spot mode and in plume mode.

II. Theory

A. Ionization Mode Theory

From Ref. 23, we have previously shown that the ionization instability associated with the plume mode has an onset criterion

$$\omega_i = \gamma_{ion} \left(\frac{2\gamma_{IAT}}{\gamma_{ion}} - 1 \right), \quad (1)$$

where γ_{IAT} is the growth rate of the ion acoustic turbulence and $\gamma_{ion} = T_e \partial \nu_{ion} / \partial T_e$ is the response of ionization to changes in temperature. Physically, this mode onsets when non-classical heating from ion acoustic waves exceeds cooling by ionization. This physical picture and instability criterion has been shown to hold when the oscillations in discharge current are relatively low compared to their mean value and are thought to transition to a nonlinear regime when discharge current oscillations are large. Experimentally, this wave can onset when the propellant flow rate to the cathode is reduced. We can reformulate this instability criterion as

$$2\omega_0 n m_i \frac{I_{dc} A_o L}{I_{th} \dot{m}} > 1, \quad (2)$$

where ω_0 is average frequency of the turbulence, n is the plasma density, m_i is the ion mass, A_o is the orifice area, L is a characteristic length scale, I_{dc} is the discharge current, I_{th} is the thermal current of the plasma, and \dot{m} is the propellant flow rate. The real frequency is given by

$$\omega_r = \sqrt{\frac{\gamma_{ion} \gamma_{IAT}}{2}}, \quad (3)$$

and is typically on the order of 10-100 kHz. This solution for the instability is found in the frame of the ions and is Doppler shifted by the ion drift velocity and as such the wave propagates from the cathode to the anode. We therefore also refer to this instability as a longitudinal ionization mode in the cathode plume.

B. Anti-drift instability

The anti-drift instability is a rotating plasma wave that is excited by the energy held in a density gradient, transverse to the magnetic field in the presence of electron collisions. The key plasma properties of the cathode plume that enable the growth of this mode are 1) that $\Omega_i < \nu_e < \Omega_e$, where $\Omega_{e,i}$ are the cyclotron frequencies of the electrons and ions, respectively; 2) the ions are cold, i.e. $T_e \gg T_i$; 3) the wave frequency is $\nu_i < \omega < \nu_e$, where $\nu_{e,i}$ are the electron and ion collision frequencies; 4) the phase velocity of in the longitudinal direction is much greater than the sound speed ($\omega/k_z \gg c_s$). Following the work in Ref. 24, the dispersion relation for these modes in a Cartesian framework is given by

$$0 = -\frac{k_x \nu^* + i\nu_{pl}}{\omega - k_x v_{E \times B} - k_z u_{e,z} + i\nu_{pl}} + \frac{T_e}{m_i} \left(\frac{k}{\omega - \vec{k} \cdot \vec{u}_i} \right)^2, \quad (4)$$

where k_x is the azimuthal wave vector, $\nu^* = T_e / B_0 n'_e / n_e$ is the diamagnetic drift, $\nu_{pl} = k_z^2 q T_e / m_e / \nu_e$. Here, we note that the expression in Eqn. 4 we have neglected magnetic gradient driven drifts (in comparison with Ref. 25) and that $k_x = m/R$, where $m = 0, 1, 2, \dots$ is the azimuthal mode number and R is the radius. This type of instability has been shown to exist in the partially magnetized hollow cathode plumes of Hall thrusters and should be present during standalone testing of a magnetic field.²²

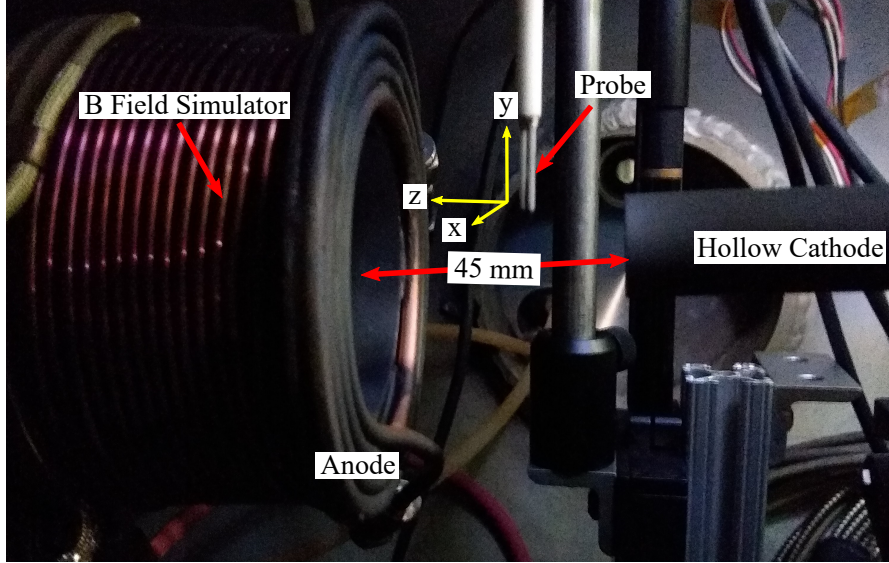


Fig. 1 Experimental setup showing the cathode, anode, wave probe, and B field simulator.

III. Experimental Methods

Experimentally, we are examining the claim from Ref. 26 that the rotating instability that forms in the presence of a magnetic field is the same as the ionization instability associated with the plume mode. To shed some light on this topic, we have designed our experiment to operate the cathode in spot mode, where the ionization wave does not dominate, and in plume mode, where the ionization-type instability is present. Then we impose an axial magnetic field with a solenoid and vary its strength. In practice, we used a LaB_6 hollow cathode that was operated on xenon at 35 A of discharge current at 12 and 5.5 sccm. The respective discharge voltage of each condition was 12.6 and 31 V. When the magnetic field is applied, the discharge voltage of both conditions rises to 25.4 V for the high flow and 40 V for the low flow conditions. The anode was positioned 45 mm downstream of the keeper exit. The anode is wrapped with a solenoid to apply an approximately axial magnetic field to the cathode plasma. The current to the solenoid was varied from 0 to 10 A. The maximum magnetic field produced is on the order of half of the field generated in the cathode region by a state of the art Hall thruster. The discharge was established in a $0.5 \text{ m} \times 1 \text{ m}$ vacuum chamber that is cryogenically pumped and achieves a base pressure of $0.12 \mu\text{Torr}$. At our selected operating conditions, the operating pressures is 50 and $27 \mu\text{Torr}$. We made our measurements of plasma waves using a wave probe, biased at -54 V to collect the ion saturation current fluctuation at 20 MHz with an oscilloscope. The axis convention is shown in green on Fig. 1, where x , y , and z are the azimuthal, radial, and axial directions, respectively. The probe was positioned at a fixed location, 7 mm radially and 20 mm downstream of the keeper exit. The experimental configuration is shown in Fig. 1.

IV. Experimental Results

In this section, we present our experimental results for the high (spot mode) and low (plume mode) flow rate conditions with variable magnetic field. First we examine the spot mode condition, primarily focusing on the presence of quasi-coherent structures that form when a magnetic field is applied. Then we discuss the plume mode condition, where the ionization instability is apparent.

A. Spot Mode

In this section we will focus the behavior of plasma oscillations in spot mode with increasing magnetic field. In Fig. 2a, we show the logarithm of the amplitude of each mode in the plasma as a function of magnetic field strength. This figure shows that at low magnetic field, there are few low-frequency oscillations at $f = 25$ and 54 kHz. With greater B , the entire spectrum rises and some large amplitude, quasi-coherent, structures are induced. The formation of this low-frequency oscillation is consistent with the previous observations of the cathode “spoke” structure that is believed to be the result of the gradient driven anti-drift instability. Fig. 2a also indicates the presence of high-frequency turbulence. When the magnetic field is off, we waves that are consistent with the presence of IAT. These modes appear to be damped out with increasing magnetic field, then a new set of waves reappears at around $B = 0.5B_{max}$. This trend is better shown by Fig. 2b where we have estimated the energy in the high-frequency broadband oscillations as $W \sim \sum_f (\tilde{i}_{sat}/i_{sat,0})$, where $100 \text{ kHz} < f < 4000 \text{ kHz}$. Along with this trend we also find that the frequency of these modes steadily decreases with magnetic field.

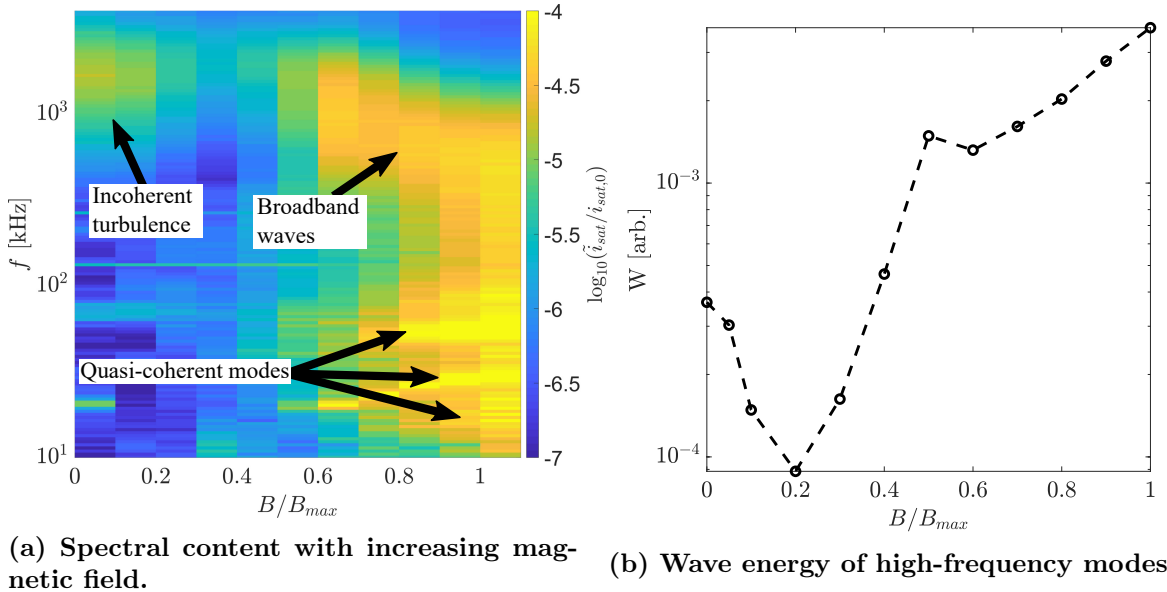


Fig. 2 Wave properties of the cathode plasma in spot mode.

To more clearly identify any axial or rotating modes, we must determine the direction of propagation of these waves. Wave propagation can be assessed by measuring the dispersion and calculating the phase velocity and examining its axial and azimuthal components. We determine the plasma dispersion using a pair of ion saturation probes, following the Beall estimation technique.^{2,27,28} Given a known separation between the probes, Δx , we calculate the phase difference and corresponding wave vector for each frequency in the Fourier spectrum as

$$k(\omega) = \frac{1}{\Delta x} \tan^{-1} \left(\frac{\Im(\mathcal{F}(\tilde{i}_{sat,2})\mathcal{F}^*(\tilde{i}_{sat,1}))}{\Re(\mathcal{F}(\tilde{i}_{sat,2})\mathcal{F}^*(\tilde{i}_{sat,1}))} \right), \quad (5)$$

where \mathcal{F} indicates a Fourier transform, \Re and \Im designate the real and imaginary parts, respectively, and $\tilde{i}_{sat,1}$ and $\tilde{i}_{sat,2}$ are the measured relative ion saturation current traces from probes 1 and 2, respectively. We calculate k over 2000 times and populate a histogram to statistically represent the dispersion, $S(\omega, k)$. We note that experimentally this probe technique is subject to aliasing when the wavelength of the wave is smaller than the distance between the probes ($\Delta x = 1.5 \text{ mm}$). This can

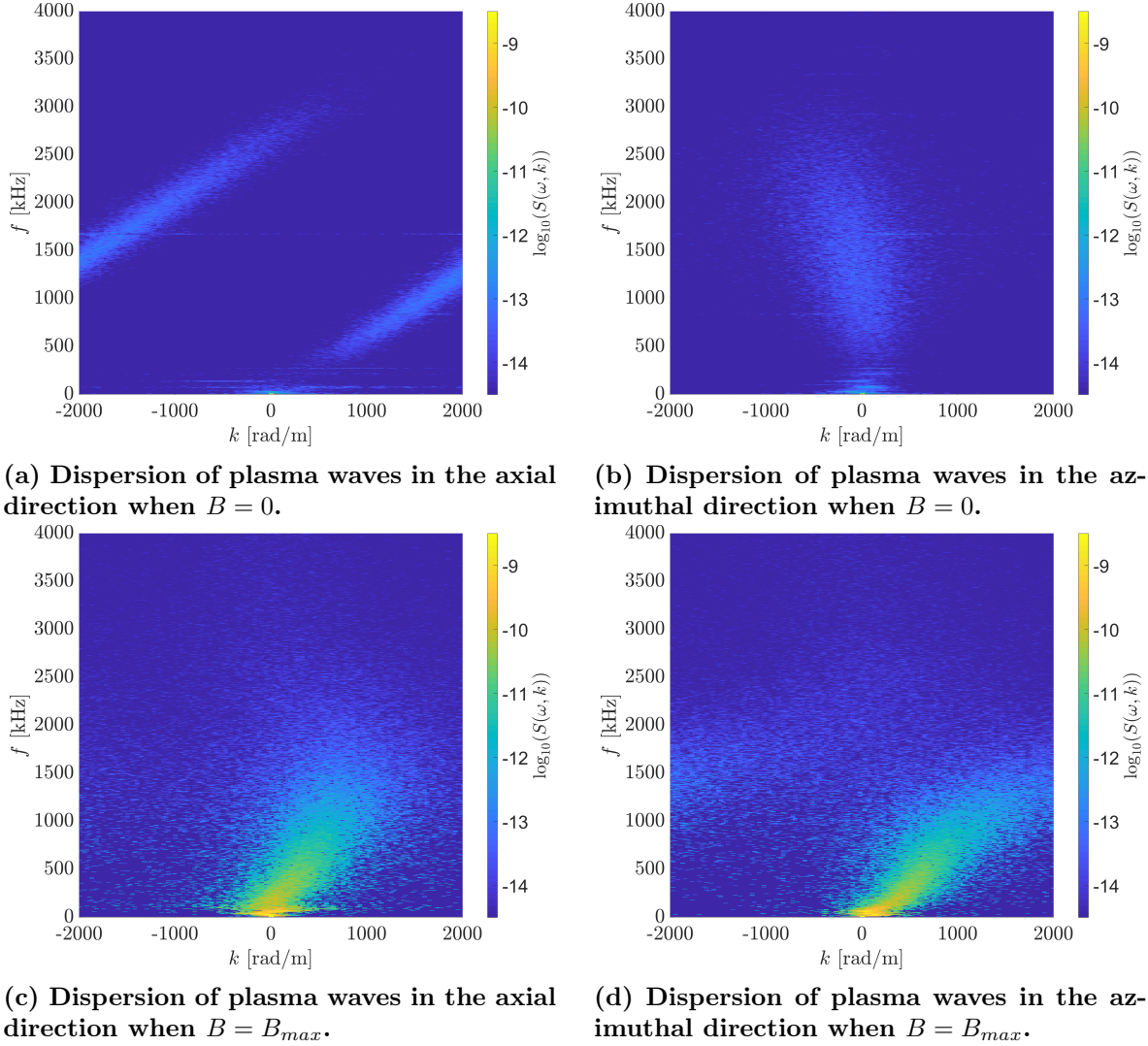


Fig. 3 The dispersion of the plasma in spot mode measured 7 mm radially and 20 mm axially downstream of the keeper exit.

result in spurious, negative wave vectors when the true wave vector is larger than $k_{max} = \pi/\Delta x \sim 2100$ [rad/m]. By examining trends in the data, we infer these smaller wavelengths.

Figure. 3 shows the dispersion of the plasma measured in the spot mode condition at low and high magnetic field settings. Figures. 3a and 3b are the dispersion when $B = 0$ in the axial and azimuthal direction, respectively. In the axial direction, we observe some waves (500 - 1000 kHz) that follow a linear dispersion relation ($\omega \propto k$), consistent with IAT. The waves at higher frequency and negative k (1000 - 3000 kHz) are the result of the previously discussed probe aliasing and continue on the trend of the lower frequency waves. In the azimuthal direction (Fig. 3b), these higher-frequency waves have some dispersion but are generally centered around $k = 0$ indicating that the waves do not primarily propagate in this direction. Figures. 3c and 3d show the dispersion for the maximum magnetic field condition. In this case, we see that the spectrum has moved to lower frequencies and longer wavelengths as well as having increased in amplitude. Furthermore, we find that with the applied magnetic field, the waves are dispersed in both the axial and azimuthal directions. This result indicates that these waves propagate in both directions, evolving helically in the plasma.

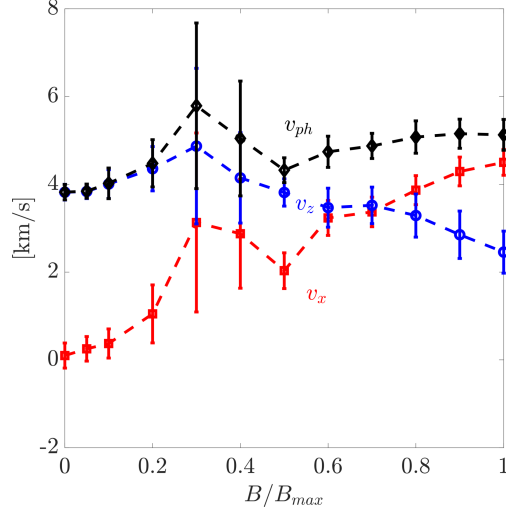


Fig. 4 Phase velocity and components of the high-frequency, broadband modes as a function of magnetic field.

From these measurements of the dispersion, we can calculate an average wave vector \bar{k} as

$$\bar{k}(\omega) = \frac{\int_{-k_{max}}^{k_{max}} k S(\omega, k) dk}{\int_{-k_{max}}^{k_{max}} S(\omega, k) dk}. \quad (6)$$

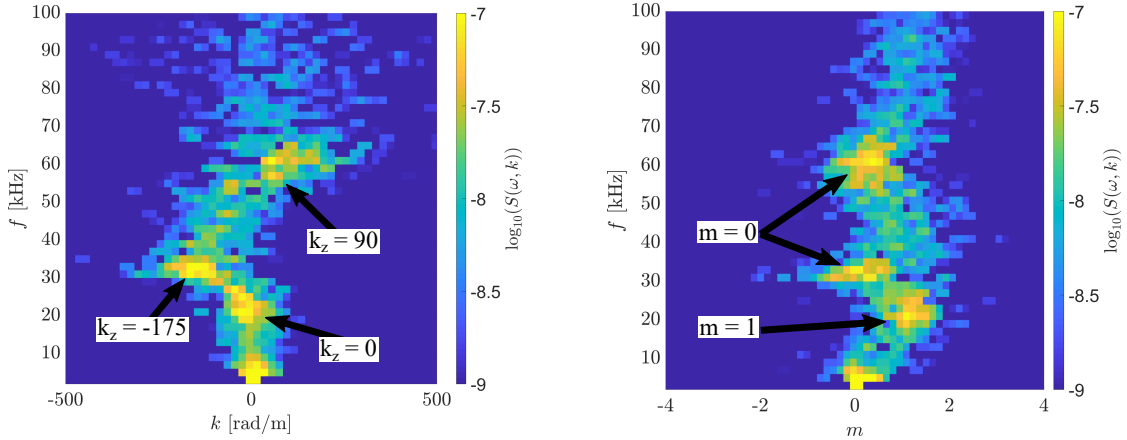
Using this value, we can determine the components of the phase velocity to be

$$v_z = \frac{\omega}{\bar{k}_z^2 + \bar{k}_x^2} \bar{k}_z, \text{ and } v_x = \frac{\omega}{\bar{k}_z^2 + \bar{k}_x^2} \bar{k}_x, \text{ and } v_{ph} = \sqrt{v_x^2 + v_z^2}. \quad (7)$$

Here, we have assumed negligible propagation in the radial direction (y). For these higher frequency modes (> 100 kHz), in Fig. 4 we plot the phase velocity and its components as a function of magnetic field. At low magnetic fields, we see that the phase velocity is dominated by the axial propagation of waves i.e. the x component of the velocity is small compared to z . In this case, $v_{ph} \sim 4$ km/s, which is consistent with previous measurement of IAT in hollow cathodes.^{2,5} At higher magnetic fields, we find that the axial velocity decreases and the azimuthal increases while the total phase velocity is approximately constant. This result suggests that by increasing the magnetic field, that the high-frequency turbulence changes from a purely longitudinal phenomenon to a rotating one.

In combination, Figs. 2 - 3 indicate the following physical picture for a spot mode discharge. When no magnetic field is present, IAT propagates longitudinally in the plume. As the magnetic field is applied, electrons begin to rotate in the plasma and the IAT is damped out and is replaced with broadband rotating modes at lower frequency and longer wavelength.

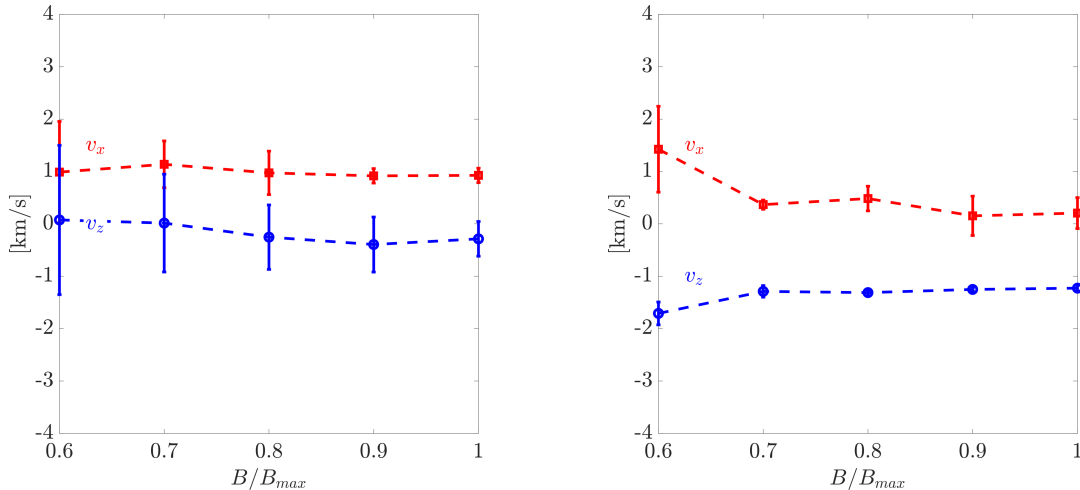
Now, up until this point we have focused our analysis on these high-frequency modes that are associated with electrostatic turbulence. At lower frequencies in Fig. 2a, we observed low-frequency structures. Zooming into our previous plots of the dispersion, we show in Fig. 5a and 5b the axial and azimuthal dispersion of these three modes. We find that at 20 kHz, we have an $m = 1$ mode that rotates and an $m = 0$ (30 kHz and second harmonic) mode that propagates axially. Examining the azimuthal mode more closely, we can plot its phase velocity as a function of magnetic field strength. Figure 6 shows the results of this calculation at magnetic field conditions where this oscillation is clearly present in the Fourier transform in Fig. 2a. The phase velocity is constant at around $v_x \sim 1$ km/s and $v_z \sim 0$ km/s. This velocity is near the ion sound speed, $c_s = \sqrt{(T_e/m_i)} \sim 1.2$ km/s for



(a) Axial dispersion of low frequency modes, $B = B_{max}$ (b) Azimuthal dispersion of low frequency modes, $B = B_{max}$

$T_e \sim 2$ eV. This azimuthally propagating wave is in qualitative agreement with previous observations in the cathode plume of Hall thrusters.²²

Now we turn to the $m = 0$ mode (30 kHz) and its harmonic (60 kHz) that are propagating longitudinally. Physically, the presence of the second harmonic indicates that this wave exhibits non-sinusoidal behavior. The modes appear to be able to propagate toward ($k_z < 0$) and away from ($k_z > 0$) the cathode based on the dispersion in Fig. 5a. Examining the phase velocity of the first harmonic, we find that it is primarily propagating in the axial direction at around 1 km/s towards the anode and its velocity is insensitive to the magnetic field. Lastly, recall from Fig. 2a, that we see that these modes are increasing in strength with magnetic field. Therefore, the magnetic field does not affect the propagation characteristics but influences the strength of this longitudinal mode. However, it remains unclear if the magnetic field plays an important role in the onset, or rather if it changes the plasma properties such that another axial instability can form in this same frequency range.



(a) Phase velocity and components of the $m = 1$ mode a function of magnetic field. (b) Phase velocity and components of the $m = 0$ mode a function of magnetic field.

Fig. 6 Phase velocity of low frequency structures.

To summarize our findings for this operating condition, there exist both azimuthal and longitudi-

nal modes that are excited in the presence of the magnetic field. The rotating modes are qualitatively similar to previous measurements of anti-drift modes in partially magnetized cathode plumes. The excitation of these axial modes is not predicted by this theory and it is unclear whether the magnetic field itself is playing an important role in the onset of this mode, or if it simply changes the plasma properties such that an axial mode, like an ionization instability, can be excited.

B. Plume Mode

In this section, we replicate a similar analysis as in Sec. A examining the wave properties as a function of magnetic field strength. Figure 7a shows that there two classes of waves in the plasma, a coherent low-frequency oscillation at 82 kHz and high-frequency, broadband waves. This quasi-coherent mode is an ionization instability that is thought to be driven by the presence of high-frequency turbulence. Figures 7a and 7b indicate that the ionization oscillation appears to decrease in amplitude with increasing magnetic field. This trend is further shown by plotting the peak amplitude of this wave as a function of magnetic field in Fig. 7c. Physically, it appears that the ionization instability damps as the magnetic field is increased. This result is in kind with previous experimental work on this instability.¹⁵

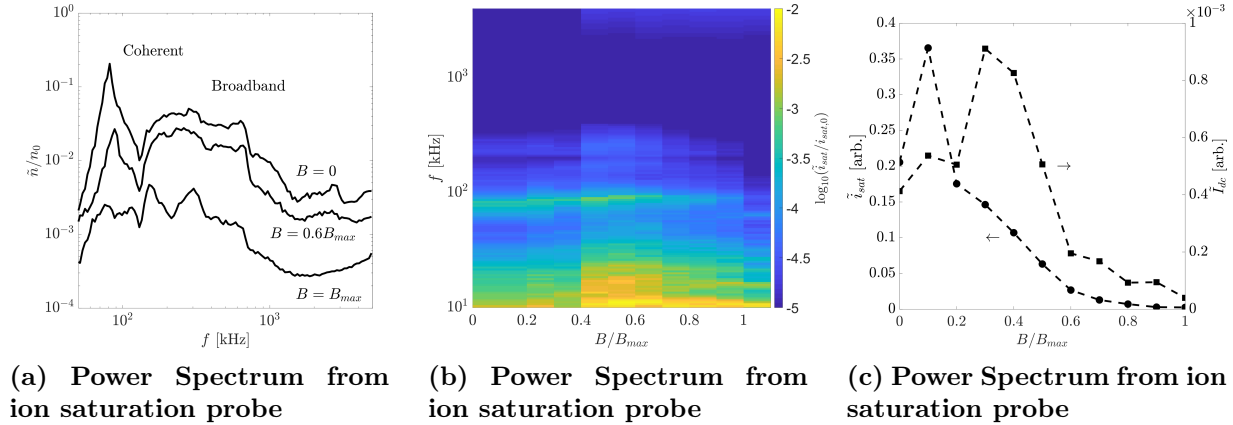
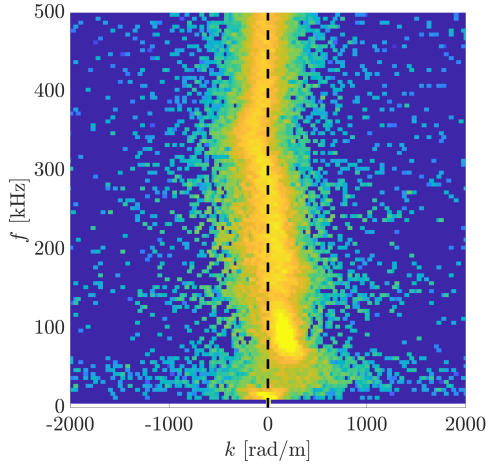


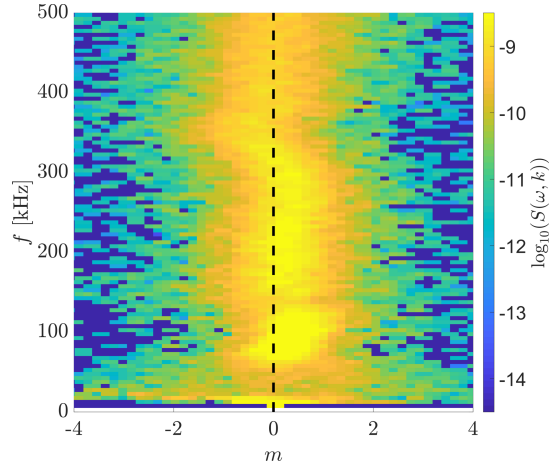
Fig. 7 Plume mode wave properties measured 7 mm radially and 20 mm downstream.

While Figs. 7a-7c show that the oscillation is damped by the presence of the magnetic field, it remains to be seen if it rotates, like the structures shown in Figs. 2 - 6a. We conduct a similar analysis to Sec. A, by first calculating the dispersion via the Beall estimation technique. The results of this analysis are shown in Figs. 8a - 8d. At low magnetic field, we find that the low-frequency wave (82 kHz) moves in towards the anode ($k > 0$) and exhibits no rotation i.e. $m \sim 0$. The broadband modes above 150 kHz are generally centered around $k = 0$ indicating that they do not propagate. In previous measurements of this instability,¹¹ the dispersion shows that these waves are IAT, however this new measurement is in a more extreme ($\sim 100\%$ peak-to-peak I_{dc} oscillations) condition where perhaps the correlation between modes is somehow broken due to the fluctuations of the plasma parameters on the low-frequency time-scale. In the high magnetic field setting, we find that the high-frequency modes have begun to rotate as in the spot mode condition, however the quasi-coherent oscillation remains at $m = 0$.

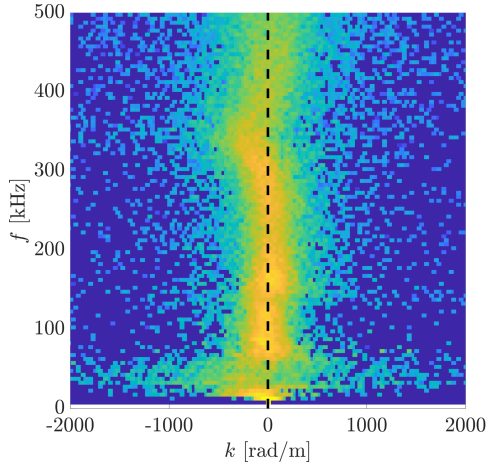
Looking at this in more detail, we use the dispersion to calculate the phase velocity of the low-frequency wave. We show in Fig. 9 the propagation of the ionization instability. Here, we see that at low magnetic field, the instability propagates purely in the axial direction ($v_x = 0$) towards the anode. As we increase the magnetic field, we find that the instability changes its direction of propagation towards the cathode. In this transition region ($B = 0.2 - 0.4B_{max}$), the mode appears to rotate very



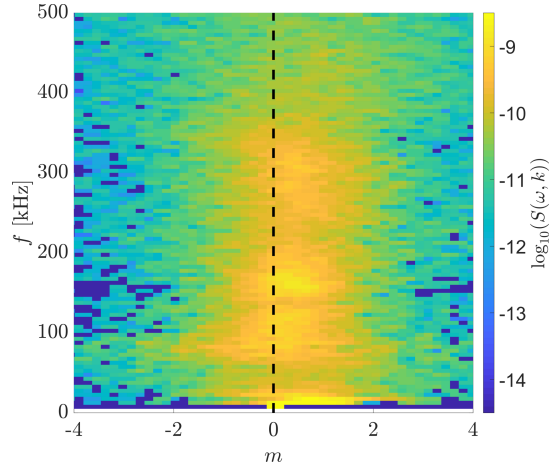
(a) Dispersion of plasma waves in the axial direction when $B = 0$.



(b) Dispersion of plasma waves in the azimuthal direction when $B = 0$.



(c) Dispersion of plasma waves in the axial direction when $B = B_{max}$.



(d) Dispersion of plasma waves in the azimuthal direction when $B = B_{max}$.

Fig. 8 The dispersion of the plasma in plume mode measured 7 mm radially and 20 mm axially downstream of the keeper exit. The vertical dashed line marks $k = 0$ or $m = 0$.

quickly, however note that in Eqn. 7 when k_z and $k_x \rightarrow 0$, then v_z and $v_x \rightarrow \infty$. As a result, our analysis technique can lead to spuriously large phase velocities when k is small and this is likely what is happening in this transition region of the plot. At higher magnetic fields, the mode moves in the axial direction back towards the cathode with little to no rotation ($v_x \sim 0$). The ionization instability is a localized phenomenon in the plume, from which plasma waves emanate towards the cathode and anode.^{10,21} The change in propagation direction is likely due to shifting of the characteristic "ionization zone" towards the anode, such that we measure the cathode-propagating wave.

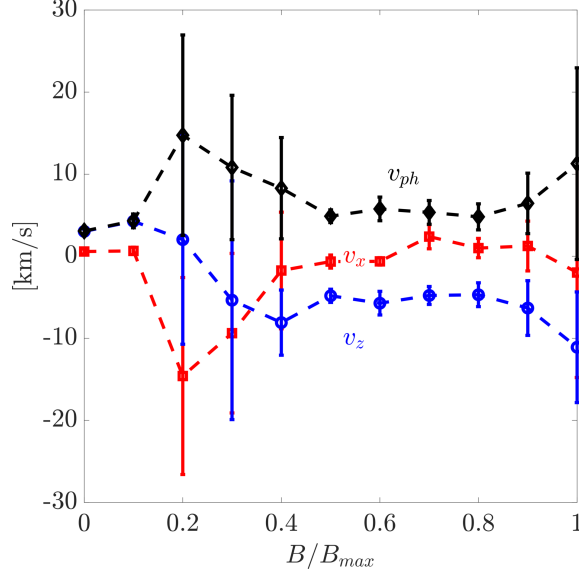


Fig. 9 Velocity of the ionization instability.

In sum, the ionization mode remains an purely axial and is damped by increasing magnetic field. No rotational modes were observed in this condition, but this could be due to the maximum magnetic field we were able to experimentally impose on the system. The behavior of the ionization instability, is distinctly different from the coherent rotational mode that onset at the higher flow rate condition.

V. Discussion

In this section, we focus our discussion on the quasi-coherent structures that form in the cathode plume. First, let us examine the rotating instability observed at the higher flow rate, spot mode condition. Similar structures have been observed previously in Hall thruster cathode plumes and have been described with the anti-drift wave theory similar to that presented in Sec. B. If we take the limit of weak magnetic field, then the dispersion reduces to

$$\omega = k \cdot (c_s + u_i) \sqrt{\frac{v^*}{v_{E \times B}}} . \quad (8)$$

By further assuming the plasma approximately follows a Boltzmann relationship with negligible temperature gradients, then $T_e \nabla n/n = E$ and we arrive at a simplified expression for the dispersion

$$\omega \simeq k \cdot (c_s + u_i) . \quad (9)$$

In the azimuthal direction, $u_i = 0$ therefore we expect phase velocity in this direction to be on the order of the ion sound speed. Without a measurement of the electron temperature, we are forced to

Table 1 Evaluated onset criterion from Eqn. 2. A value > 1 implies the onset criterion is met for the turbulence-driven ionization instability.

Condition	Spot	Plume
$B = 0$	0.8	1.3
$B = B_{max}$	0.14	1.35

make an estimate based on previous work to evaluate the dispersion. Most measurements of cathodes show that the electron temperature is typically between 1 and 5 eV. Given this assumption and the dispersion relation, we find that the velocity should lie around 1.4 ± 0.5 km/s. Experimentally we find that once this wave is excited, its velocity does not vary with the magnetic field. This result is consistent with the theory, since the ratio $v^*/v_{E \times B}$ is independent of the applied field. The anti-drift wave model for this structure also predicts that there should be a small axial component, which our technique cannot distinguish from $k_z = 0$.

Now we transition our discussion to a comparison of quasi-coherent oscillation in plume mode with the structures that formed in spot mode. First we evaluate the onset criterion in Eqn. 2 for the ionization instability for each condition (spot and plume mode, $B = 0$ and $B = B_{max}$) to determine if this kind phenomenon could possibly drive the structures we observe. In this experiment, we were unable to measure all the background plasma parameters; however, we can use estimates from the literature to determine if the trends appear correct. From Ref. 29, the plasma density at the orifice can be as large as 10^{22} m⁻³ and the temperature is around 1 eV. Note that the fundamental onset criterion depends exponentially on temperature and as such this is a large source of uncertainty in our analysis. The keeper orifice is used as the characteristic area and the cathode-to-anode separation for the characteristic length. We calculate the average frequency of the turbulence as $\omega_0 = \int_{\omega} \omega (\tilde{\phi}/T_e)^2 d\omega / \int_{\omega} (\tilde{\phi}/T_e)^2 d\omega$. Evaluating the onset criterion with these approximate values, we find in Tab. 1 that the ionization mode is damped in the spot mode conditions but should likely be growing in the plume mode conditions. This result suggests that it is unlikely that the ionization mode is forming, even under the presence of the magnetic field.

Further contrasting these modes, we see experimentally that in plume mode we find that the axial ionization wave is damped by the magnetic field (Fig. 7c, a distinctly different behavior from the azimuthal and longitudinal modes that grow in with increasing magnetic field (Fig. 2a). Furthermore, these instabilities travel at different speeds, with the rotating and axial structures in spot mode propagate at $\mathcal{O}(1$ km/s) while the ionization mode is at $\mathcal{O}(10$ km/s). Although these modes exist in the same frequency band, given the evaluation of the onset criterion in Tab. 1, the disparity in their propagating characteristics, and behavior with an applied magnetic field, we conclude that these coherent structures that emerge in the cathode plume are separate phenomena, in contrast with the interpretation of recent numerical simulations of these cathodes.²⁶ In fact, after examining the fundamental onset criterion in Eqn. 1 it is unclear what the source of energy could be to drive the ionization mode unstable in the azimuthal direction.

VI. Conclusions

In conclusion, we have measured plasma waves in the cathode plume in the spot and plume mode conditions. Initially in spot mode, we measured ion acoustic turbulence. By varying the magnetic field, we can induce quasi-coherent structures that propagate in the axial and azimuthal directions. While the rotating mode is consistent with the an anti-drift wave in the low magnetic field limit, the origins of the longitudinal mode remain unclear. By increasing the magnetic field in plume mode,

where an ionization instability was initially present, we have shown that this mode can be damped. By examining the onset criterion for an ionization-type wave and the propagation of these instabilities, we determined that the structures formed in plume mode are different from the ionization instability in plume mode, in contrast to recent numerical simulations.

Acknowledgements

This work was funded by the NASA Space Technology Research Fellowship under grant number NNX15AQ37H.

References

- [1] Ioannis G. Mikellides, Ira Katz, Dan M. Goebel, and Kristina K. Jameson. Evidence of nonclassical plasma transport in hollow cathodes for electric propulsion. *Journal of Applied Physics*, 101(6):063301, March 2007. ISSN 0021-8979. doi: 10.1063/1.2710763. URL <http://aip.scitation.org/doi/abs/10.1063/1.2710763>.
- [2] Benjamin A. Jorns, Ioannis G. Mikellides, and Dan M. Goebel. Ion acoustic turbulence in a 100-A LaB6 hollow cathode. *Physical Review E*, 90(6):063106, December 2014. doi: 10.1103/PhysRevE.90.063106. URL <http://link.aps.org/doi/10.1103/PhysRevE.90.063106>.
- [3] Alejandro Lopez Ortega, Ioannis G. Mikellides, and Benjamin Jorns. First-principles modeling of the IAT-driven anomalous resistivity in hollow cathode discharges II: Numerical simulations and comparison with measurements. American Institute of Aeronautics and Astronautics, July 2016. ISBN 978-1-62410-406-0. doi: 10.2514/6.2016-4627. URL <http://arc.aiaa.org/doi/10.2514/6.2016-4627>.
- [4] Benjamin Jorns, Alejandro Lopez Ortega, and Ioannis G. Mikellides. First-principles Modelling of the IAT-driven Anomalous Resistivity in Hollow Cathode Discharges I: Theory. American Institute of Aeronautics and Astronautics, July 2016. ISBN 978-1-62410-406-0. doi: 10.2514/6.2016-4626. URL <http://arc.aiaa.org/doi/10.2514/6.2016-4626>.
- [5] Benjamin A. Jorns, Christopher Dodson, Dan M. Goebel, and Richard Wirz. Propagation of ion acoustic wave energy in the plume of a high-current LaB6 hollow cathode. *Physical Review E*, 96(2):023208, August 2017. doi: 10.1103/PhysRevE.96.023208. URL <https://link.aps.org/doi/10.1103/PhysRevE.96.023208>.
- [6] Gaétan Sary, Laurent Garrigues, and Jean-Pierre Boeuf. Hollow cathode modeling: I. A coupled plasma thermal two-dimensional model. *Plasma Sources Science and Technology*, 26(5):055007, 2017. ISSN 0963-0252. doi: 10.1088/1361-6595/aa6217. URL <http://stacks.iop.org/0963-0252/26/i=5/a=055007>.
- [7] Christopher Dodson, Benjamin A. Jorns, and Richard E. Wirz. Measurements of ion velocity and wave propagation in a hollow cathode plume. *Plasma Sources Science and Technology*, 2019.
- [8] Gaétan Sary, Laurent Garrigues, and Jean-Pierre Boeuf. Hollow cathode modeling: II. Physical analysis and parametric study. *Plasma Sources Science and Technology*, 26(5):055008, 2017. ISSN 0963-0252. doi: 10.1088/1361-6595/aa6210. URL <http://stacks.iop.org/0963-0252/26/i=5/a=055008>.
- [9] Ioannis G. Mikellides, Pablo Guerrero, Alejandro Lopez Ortega, and James E. Polk. Spot-to-plume Mode Transition Investigations in the HERMeS Hollow Cathode Discharge Using Coupled 2-D Axisymmetric Plasma-Thermal Simulations. American Institute of Aeronautics and Astronautics, July 2018. ISBN 978-1-62410-570-8. doi: 10.2514/6.2018-4722. URL <https://arc.aiaa.org/doi/10.2514/6.2018-4722>.
- [10] Marcel P. Georjin, Benjamin A. Jorns, and Alec D. Gallimore. Correlation of ion acoustic turbulence with self-organization in a low-temperature plasma. *Physics of Plasmas*, 26(8):082308, August 2019. ISSN 1070-664X. doi: 10.1063/1.5111552. URL <https://aip.scitation.org/doi/full/10.1063/1.5111552>.

- [11] Marcel P. Georjin, Benjamin Jorns, and Alec Gallimore. Time-varying Non-classical Collisions and Turbulence in a Hollow Cathode. In *AIAA Propulsion and Energy 2019 Forum*, Indianapolis, IN, August 2019. American Institute of Aeronautics and Astronautics. ISBN 978-1-62410-590-6. doi: 10.2514/6.2019-4079. URL <https://arc.aiaa.org/doi/10.2514/6.2019-4079>.
- [12] George A. Csiky. Measurements of some properties of a discharge from a hollow cathode. *NASA Technical Note*, 1969. URL <https://ntrs.nasa.gov/archive/nasa/casi.ntrs.nasa.gov/19690008515.pdf>.
- [13] C.M. Philip. A Study of Hollow Cathode Discharge Characteristics. *AIAA Journal*, 9(11):2191–2196, November 1971. ISSN 0001-1452, 1533-385X. doi: 10.2514/3.50024. URL <http://arc.aiaa.org/doi/10.2514/3.50024>.
- [14] Verlin J. Friedly and Paul J. Wilbur. High current hollow cathode phenomena. *Journal of Propulsion and Power*, 8(3):635–643, 1992. ISSN 0748-4658. doi: 10.2514/3.23526. URL <http://dx.doi.org/10.2514/3.23526>.
- [15] Dan M. Goebel, Kristina K. Jameson, Ira Katz, and Ioannis G. Mikellides. Potential fluctuations and energetic ion production in hollow cathode discharges. *Physics of Plasmas (1994-present)*, 14(10):103508, October 2007. ISSN 1070-664X, 1089-7674. doi: 10.1063/1.2784460. URL <http://scitation.aip.org/content/aip/journal/pop/14/10/10.1063/1.2784460>.
- [16] Marcel P Georjin, Benjamin A Jorns, and Alec D Gallimore. Experimental Evidence for Ion Acoustic Solitons in the Plume of a Hollow Cathode. volume 403, page 12, Sevilla, Spain, May 2018.
- [17] Sarah E. Cusson, Benjamin Jorns, and Alec Gallimore. Simple Model for Cathode Coupling Voltage Versus Background Pressure in a Hall Thruster. In *53rd AIAA/SAE/ASEE Joint Propulsion Conference*, Atlanta, GA, July 2017. American Institute of Aeronautics and Astronautics. ISBN 978-1-62410-511-1. doi: 10.2514/6.2017-4889. URL <https://arc.aiaa.org/doi/10.2514/6.2017-4889>.
- [18] Sarah E. Cusson, Benjamin A. Jorns, and Alec Gallimore. Ion Acoustic Turbulence in the Hollow Cathode Plume of a Hall Effect Thruster. In *2018 Joint Propulsion Conference*, Cincinnati, Ohio, July 2018. American Institute of Aeronautics and Astronautics. ISBN 978-1-62410-570-8. doi: 10.2514/6.2018-4509. URL <https://arc.aiaa.org/doi/10.2514/6.2018-4509>.
- [19] Dan Goebel, Kristina K. Jameson, and Richard R. Hofer. Hall Thruster Cathode Flow Impact on Coupling Voltage and Cathode Life. *Journal of Propulsion and Power*, 28(2):355–363, March 2012. ISSN 0748-4658, 1533-3876. doi: 10.2514/1.B34275. URL <http://arc.aiaa.org/doi/10.2514/1.B34275>.
- [20] Marcel Georjin, Christopher Durot, and Alec D. Gallimore. Preliminary Measurements of Time-Resolved Ion Velocity Distributions Near a Hollow Cathode. 2015. URL <http://www.umich.edu/~peplweb/pdf/IEPC-2015-106.pdf>.
- [21] Marcel P. Georjin, Benjamin A. Jorns, and Alec D. Gallimore. An Experimental and Theoretical Study of Hollow Cathode Plume Mode Oscillations. volume IEPC-2017-298, Atlanta Georgia, October 2017. Electric Rocket Propulsion Society.
- [22] Benjamin A. Jorns and Richard R. Hofer. Low Frequency Plasma Oscillations in a 6-kW Magnetically Shielded Hall Thruster. In *49th AIAA/ASME/SAE/ASEE Joint Propulsion Conference*. American Institute of Aeronautics and Astronautics, 2013. URL <http://arc.aiaa.org/doi/abs/10.2514/6.2013-4119>.
- [23] Marcel P. Georjin, Benjamin A. Jorns, and Alec D. Gallimore. Onset criterion for a turbulence-driven ionization instability in hollow cathodes. volume 155, Vienna, Austria, 2019. Electric Rocket Propulsion Society.
- [24] Benjamin A. Jorns, Sarah E. Cusson, Zachariah Brown, and Ethan T. Dale. Non-classical Electron Transport in the Cathode Plume of a Hall Effect Thruster. *Physics of Plasmas -Submitted*, 2019.

- [25] Winston Frias, Andrei I. Smolyakov, Igor D. Kaganovich, and Yevgeny Raitses. Long wavelength gradient drift instability in Hall plasma devices. I. Fluid theory. *Physics of Plasmas*, 19(7):072112, July 2012. ISSN 1070-664X. doi: 10.1063/1.4736997. URL <https://aip.scitation.org/doi/abs/10.1063/1.4736997>.
- [26] Ioannis G. Mikellides, Alejandro Lopez Ortega, Dan M. Goebel, and Giulia Becatti. Dynamics of a Hollow Cathode Discharge in the Frequency Range of 1-500 kHz. *Plasma Sources Science and Technology* - Submitted, 2019.
- [27] Dragan B. Ilić. Measurement of Ion-Acoustic Plasma Turbulence by Cross-Power Spectra. *Physical Review Letters*, 34(8):464–466, February 1975. ISSN 0031-9007. doi: 10.1103/PhysRevLett.34.464. URL <https://link.aps.org/doi/10.1103/PhysRevLett.34.464>.
- [28] J. M. Beall, Y. C. Kim, and E. J. Powers. Estimation of wavenumber and frequency spectra using fixed probe pairs. *Journal of Applied Physics*, 53(6):3933–3940, June 1982. ISSN 0021-8979. doi: 10.1063/1.331279. URL <http://aip.scitation.org/doi/abs/10.1063/1.331279>.
- [29] Dan M. Goebel and Ira Katz. *Fundamentals of electric propulsion: ion and Hall thrusters*, volume 1. John Wiley & Sons, 2008. URL [http://books.google.com/books?hl=en&lr=&id=P50GFXcBKcW&oi=fnd&pg=PR5&dq=%22Electrode+Breakdown%22+%226:+Hollow%22+%22Ionization+Length+and+Scaling%22+%22Dielectric-Wall+Versus+Metallic-Wall+Comparison%22+%22Dispenser+Cathodes+in+Insert%22+%22Hall+Thruster%22+%22Pyrolytic+Graphite%22+%22Hollow+Cathode+Operation%22+%22TAL+Hall+Thruster+Efficiency+\(Metallic+Walls&ots=Sbv2zvFn6h&sig=jItSQ0scncTmqCz26jx_rAYmlbc](http://books.google.com/books?hl=en&lr=&id=P50GFXcBKcW&oi=fnd&pg=PR5&dq=%22Electrode+Breakdown%22+%226:+Hollow%22+%22Ionization+Length+and+Scaling%22+%22Dielectric-Wall+Versus+Metallic-Wall+Comparison%22+%22Dispenser+Cathodes+in+Insert%22+%22Hall+Thruster%22+%22Pyrolytic+Graphite%22+%22Hollow+Cathode+Operation%22+%22TAL+Hall+Thruster+Efficiency+(Metallic+Walls&ots=Sbv2zvFn6h&sig=jItSQ0scncTmqCz26jx_rAYmlbc).